

Precision standard siren cosmology

Hsin-Yu Chen^{1,2}, Maya Fishbach¹ and Daniel E. Holz^{1,3}

¹*Department of Astronomy and Astrophysics,
University of Chicago, Chicago, Illinois 60637, USA*

²*Black Hole Initiative
Harvard University, Cambridge,
Massachusetts 02138, USA*

³*Enrico Fermi Institute, Department of Physics,
and Kavli Institute for Cosmological Physics
University of Chicago, Chicago, Illinois 60637, USA*

We discuss the constraints on the Hubble constant to be expected from standard siren sources in ground-based gravitational wave detectors. We consider binary neutron star and binary black hole sources, and focus on the role of golden sirens (the loudest and best constrained sources) to constrain cosmological parameters. We consider two approaches: the counterpart case, where electromagnetic observations provide an independent measurement of the redshift to the sources, and the statistical case, incorporating an analysis over all potential host galaxies within the localization volumes. Our analysis includes realistic measurement uncertainties and selection biases. Although the specific results depend on the configuration and sensitivity of the detector networks, we find that the statistical method would constrain H_0 to 4% with ~ 100 detections of binary neutron star mergers, while an equivalent statistical measurement can be accomplished with ~ 30 golden events (all fractional uncertainties are quoted as half of the width of the symmetric 68% credible interval divided by the median of the H_0 posterior). Alternatively, with $\sim 10/60/200$ binary neutron star standard sirens with electromagnetic counterparts, H_0 would be constrained to 4/2/1%. Given current rate uncertainties, the 5% measurement may happen within the 9 month O3 LIGO/Virgo run (starting Fall 2018), or if the rate is low this may not happen until one full year of the LIGO/Virgo network at design sensitivity (starting $\sim 2021+$). Similarly, the 1% measurement may happen within two years of running at design sensitivity ($\sim 2024+$), or may not happen until 3+ years of operation of a full five-detector network. Although the rates, and thus precise timetable, remain uncertain, precision standard siren cosmology can be expected in the foreseeable future.

I. INTRODUCTION

With the first and second observing runs of Advanced LIGO and Virgo, the era of gravitational-wave astronomy has begun. One of the great promises of the field is the use of gravitational waves to directly measure the luminosity distance to sources, which was dramatically exemplified with the measurement of H_0 [1] from GW170817 [2]. The cosmological potential of gravitational-wave (GW) sources was first recognized by Bernard Schutz over thirty years ago [3], when he proposed that binary coalescences could be used to measure the Hubble constant, H_0 . The amplitude of the wave is inversely related to the luminosity distance, and the scaling constant can be directly inferred from the evolution of the gravitational waveform. This measurement does not entail the use of a distance ladder; the calibration is provided directly from the theory of general relativity. The redshift to the source cannot be inferred directly from the waveform, however. In [3] the redshift was determined in a statistical fashion, considering every galaxy in the localization region as a potential host and incorporating the redshift of each galaxy. By averaging over enough sources, the true value of H_0 could be inferred. Other statistical approaches utilize additional astrophysical information, such as assuming a mass distribution for the sources [4] or a determination of the equation of state of neutron stars [5]. Alternatively, in some cases it is

possible to identify an electromagnetic (EM) counterpart to the gravitational wave source, and directly measure the redshift in the electromagnetic spectrum. This was first emphasized in [6], where these sources were dubbed “standard sirens” (in comparison to their electromagnetic cousins, “standard candles”). Short gamma-ray bursts (GRBs) were subsequently suggested as ideal standard sirens [7], since they are expected to be bright in the electromagnetic spectrum and loud in the gravitational wave spectrum. GW170817 is the poster child for standard siren measurements with a counterpart [8].

There has subsequently been a large body of work exploring the power of standard sirens to measure cosmological parameters, focusing both on the counterpart case [9–14] and the statistical case [5, 12, 15–17]. In this work we focus in particular on the critical role of the “golden sirens”, the loudest [18], best localized [19] events, for which it will be easiest to identify the counterparts and/or host galaxies. We show that golden events contribute substantially to cosmological inferences, especially in the absence of a detected counterpart. Unlike previous work, we incorporate a full statistical approach, including the effects of realistic measurement uncertainties and selection biases on GW and EM observations.

In what follows we focus on the measurement of H_0 , as this parameter is of fundamental importance to cosmology [20], and is currently the subject of intense debate and scrutiny [21]. As binaries are detected to increasingly

high redshift [22, 23], the full evolution of the luminosity distance-redshift relation may be probed. We fix the cosmological parameters to their Planck values [24], allowing only H_0 to float; this can be trivially generalized when there are sufficient detections at sufficiently high redshift to constrain additional cosmological parameters. Since our simulated populations extend well into the Hubble flow, we use the full luminosity distance-redshift relation, not just the linear approximation (Eq. A16).

As discussed above, there are two basic approaches to standard siren cosmology: counterpart and statistical. In the counterpart case, electromagnetic observations identify a counterpart to the GW source. This can be done by directly observing a transient electromagnetic source, such as a gamma-ray burst/afterglow or a kilonova. The redshift can then be determined, either directly from the counterpart, or by identifying the host galaxy associated with the counterpart and measuring its redshift instead. Alternatively, if no counterpart is identified, then a statistical analysis can be performed over all galaxies within the three dimensional localization region. Each galaxy provides a value of the redshift, and therefore a posterior distribution for the Hubble constant. These need to be combined for all potential host galaxies, potentially weighting by their galaxy likelihoods (not only from the GW localization, but perhaps also factoring in additional issues such as the stellar mass or the rate of star formation). Although this may be a weak constraint on H_0 , given that there are potentially large numbers of galaxies in the localization volumes, this method will converge to the correct value of H_0 for sufficient numbers of detected events. For golden events, the localization can become small enough that only a few galaxies remain in the localization region [19]. In the extreme case of very well localized events, the single true host galaxy remains within the localization region and the statistical and counterpart cases are identical. Alternatively, if an electromagnetic counterpart is identified, but no redshift can be directly determined and no host galaxy can be associated, the sky location of the counterpart can greatly constrain the localization volume. In this case the statistical approach can be applied to a “pencil beam” of potential galaxy hosts surrounding the counterpart. For example, we can restrict our analysis to galaxies within $\lesssim 1$ Mpc of the line of sight to take into account the effect of kicks and long delay times, which can potentially lead to significant physical displacements of the binary from its host galaxy. The pencil beam volumes can be significantly smaller than the full LIGO/Virgo localization volumes, and therefore contain fewer potential host galaxies and engender improved cosmological constraints. In this paper we explore the expectations for standard siren constraints on H_0 from ground-based GW detector networks, considering both the counterpart and the statistical approaches.

II. METHODS

In what follows we present a statistical method for inferring cosmological parameters from GW and EM measurements. As described below, we Monte Carlo a representative sample of GW detections for a range of detector configurations. We then simulate the analysis of these data sets, and explore the resulting standard siren constraints. We highlight important aspects of our calculation, such as the role of peculiar velocities and selection effects. The details of our statistical approach can be found in the Appendix.

A. Synthetic Events and Host Galaxies

We consider three observing scenarios [25]: HLV at expected O3 sensitivity ($\sim 2018+$), HLV at design sensitivity ($\sim 2021+$), and HLVJI at design sensitivity ($\sim 2024+$), where H stands for LIGO-Hanford, L for LIGO-Livingston, V for Virgo, J for KAGRA, and I for LIGO-India. We explore the constraints on H_0 for each of these gravitational-wave networks.

Measuring H_0 with standard sirens relies on our ability to extract the luminosity distance and sky position of GW sources. We follow the procedure in [19] to localize synthetic binary neutron star (BNS) and binary black hole (BBH) detections. The population of binaries are distributed uniformly in comoving volume in a Planck [24] cosmology ($\Omega_{M_0} = 0.308, \Omega_{\Lambda_0} = 0.692, h_0 = 0.678$). For a given network of detectors and detector sensitivities, we then calculate the matched-filter signal-to-noise ratio (SNR) for each simulated binary. We draw the “measured” SNR from a Gaussian distribution centered at the matched-filter value with a standard deviation $\sigma = 1$. Binary mergers are detected only if their measured network SNR is greater than 12. For each detected merger, we calculate its 3D localization according to the methods in [19]. (We have verified that this procedure yields results which are consistent with the full parameter estimation pipeline, LALInference [26].) The 3D localization takes the form of a posterior probability distribution function (PDF), $p(\alpha, \delta, D_L | d_{\text{GW}})$, over the sky position (α, δ) and luminosity distance, D_L .

The gravitational wave signal from each detected binary merger provides a measurement of D_L . To calculate H_0 , we must also measure a redshift for each binary merger. Throughout, we take the redshift, z , to be the peculiar-velocity corrected redshift; that is, the redshift that the source would have if it were in the Hubble flow. We consider two cases: the redshift information either comes from a direct EM counterpart, such as a GRB/afterglow and/or a kilonova (“counterpart”), or a statistical analysis over a catalog of potential host galaxies (“statistical”).

In the counterpart case, we assume that the EM counterpart is close enough to its host galaxy so that the host can be unambiguously identified, and we can measure its

sky position and redshift. This measurement takes the form of a posterior PDF, $p(\alpha, \delta, z|d_{EM})$. We assume that the sky position of each host galaxy is perfectly measured (i.e. with negligible measurement error), meaning we can fix the source sky position to the location of the counterpart in the GW parameter estimation (rather than marginalizing over all sky positions). The GW distance posterior changes slowly over the sky and therefore is not sensitive to the precise location of the counterpart. However, since the GW sky localization areas can be very large, fixing the source position can lead to important improvements in the distance, and hence H_0 , measurements. We also assume that the peculiar-velocity corrected redshift, z , is measured with a $1\text{-}\sigma$ error of $(200 \text{ km/s})/c$, which is a typical uncertainty for the peculiar velocity correction [27, 28].

In the absence of an EM counterpart, we cannot identify a single host galaxy, and must use a catalog of all potential host galaxies [3, 17]. We assume that such a catalog is complete and contains the true host galaxy. While our method can be extended to incomplete catalogs that have a high probability of missing the correct host (as long as the completeness is understood, we will not bias the measurement), we argue that the H_0 measurement in such cases will be largely uninformative. Instead, we advocate the construction of a real-time galaxy catalog for all “golden” BNS and BBH events, which we define to be those localized to a volume (assuming Planck cosmology) less than $1,000 \text{ Mpc}^3$ for BNS and $10,000 \text{ Mpc}^3$ for BBH, and containing $\mathcal{O}(10\text{--}100)$ potential host galaxies. Depending on the observing run, $\sim 10\%/1\%/0.1\%$ of BNS/10–10 M_\odot BBH/30–30 M_\odot BBH events will be golden [19], and we can hope to survey the entire volume of interest for each of them. We show that, even with complete galaxy catalogs for all events, the golden events provide the tightest H_0 constraints in the statistical case, and contribute more significantly to the measurement than average events.

To simulate the galaxy catalogs, we construct a mock catalog by distributing galaxies uniformly in comoving volume with a number density of 0.02 Mpc^{-3} . This corresponds to the number density of galaxies 25% as bright as the Milky Way, assuming the galaxy luminosity function is described by the Schechter function [29] with B-band parameters $\phi_* = 1.6 \times 10^{-2} h^3 \text{ Mpc}^{-3}$, $\alpha = -1.07$, $L_* = 1.2 \times 10^{10} h^{-2} L_{B,\odot}$, and $h = 0.7$ (where $L_{B,\odot}$ is the solar luminosity in B-band), and integrating down to $0.16 L_*$ to find the luminosity density. (This corresponds to 83% of the total luminosity [30–32].) Thus, we assume that only galaxies brighter than $0.16 L_*$ can host binary mergers, although we note that the population of host galaxies is currently uncertain. In what follows we weight each galaxy equally, but as described in the Appendix we can also prefer galaxies with greater stellar mass or star-forming luminosity, or potentially incorporate redshift-dependent coalescence rates, by adding a factor in Eq. A3.

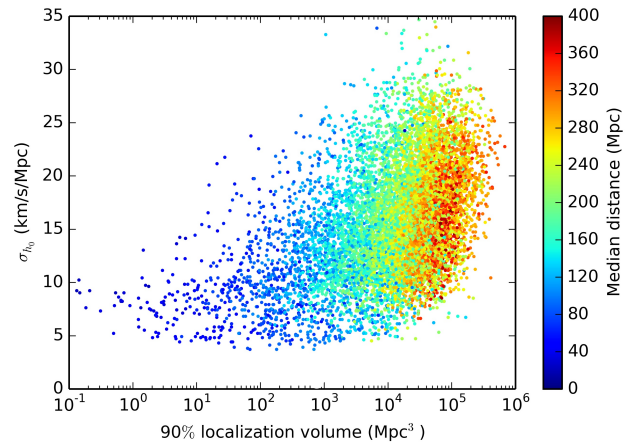


FIG. 1: H_0 uncertainty, σ_{h_0} , for BNS systems with identified counterparts (and thus redshifts) detected by the HLV network operating at design sensitivity, as a function of the 90% localization volume. The H_0 uncertainty is defined as half of the width of the symmetric 68% credible interval. The colors correspond to the median of the GW distance measurement. The lower $\sim 3 \text{ km/s/Mpc}$ limit to the precision of individual measurements is due to the “sweet spot” between peculiar velocities and distance uncertainties, as discussed in the text. We find that, in general, closer events have smaller localization volume and lead to better constraints on H_0 , although the closest events yield slightly worse constraints because of their larger fractional peculiar velocity uncertainties.

B. Golden Events

Not all GW events contribute equally to the H_0 measurements. In the counterpart case, the fractional error on the H_0 measurement from a single source depends on the fractional distance uncertainty of the GW source and the fractional redshift uncertainty of its host galaxy. To first order, this is:

$$\left(\frac{\sigma_{H_0}}{H_0} \right) \bigg|_{\text{1gal}} \approx \left(\frac{\sigma_{v_H}}{v_H} \right)^2 + \left(\frac{\sigma_{D_L}}{D_L} \right)^2, \quad (1)$$

where v_H is the peculiar-velocity corrected “Hubble velocity”. Because the recessional velocity uncertainty, σ_{v_H} , is typically around $150\text{--}250 \text{ km/s}$, the fractional recessional velocity decreases with distance. Meanwhile, the fractional distance uncertainty scales roughly inversely with SNR, and therefore tends to increase with distance. There is thus a “sweet spot”, where the peculiar velocities and the distance uncertainties are comparable; for O2 this was $\sim 30 \text{ Mpc}$, near the distance of GW170817. The sweet spot will increase as the networks become more sensitive; for detectors at design sensitivity the ideal BNS standard siren distance will be $\sim 50 \text{ Mpc}$. At distances beyond this, the distance uncertainty will tend to dominate the peculiar velocity uncertainty; in this regime, the highest SNR events tend to provide the

tightest H_0 constraints. Prior to identifying the counterpart for a particular event, we can estimate the accuracy of the H_0 measurement from the width and central value (e.g. median) of the GW distance posterior according to Eq. 1, using an estimated $v_H \approx 70 \langle D_L \rangle$ km/s/Mpc, where $\langle D_L \rangle$ is the median GW distance. (Here we must use the GW posterior marginalized over the sky position, as we do not yet know the sky position of the counterpart.) We verify that this estimate of the combined distance and redshift uncertainty is a reasonable proxy for the resulting H_0 uncertainty, assuming an EM counterpart is found and provides an independent measurement of redshift. One can then select BNS events for EM follow up based on this prediction for the H_0 uncertainty provided by the distance posterior.

In the absence of a counterpart, we cannot assign a unique host, and so the H_0 error increases with the number of potential host galaxies in the localization volume (although significant galaxy clustering can mitigate this: in the case of GW170817 the optical counterpart was found in NGC 4993, which is a member of a group of ~ 20 galaxies, all of which have an equivalent Hubble recessional velocity [33]). We refer to the events with the smallest localization volumes as “golden” events; these tend to be the nearest, highest-SNR events. Since both the localization volume and the fractional distance uncertainty scale inversely with the SNR, we expect the golden events to yield the tightest constraints in both the counterpart and statistical case. Figure 1 shows the relationship between the localization volume and the width of the H_0 measurement in the counterpart case for events detected by the HLV network. Golden events indeed yield better H_0 constraints than the average event, but we note that the relationship between localization volume and the width of the H_0 measurement is not very tight. Similarly, in the statistical case, the relationship between the localization volume and the resulting H_0 uncertainty depends on the details of the event. Two events may have the same localization volume, but one event may have a very well-constrained distance and a large sky area, whereas the other may have a well-constrained sky area but a large distance uncertainty. In this case the event with the small fractional distance uncertainty will provide the tighter constraint even though they have the same number of galaxies in the localization volume. Nevertheless, EM follow-up campaigns are more likely to identify a counterpart successfully for golden events (selected for their tight localization volume) than for an average event, especially since these events tend to be nearby, and in what follows we focus on the golden events in both the counterpart and statistical cases.

III. RESULTS

We carry out the analysis described in the previous section for simulated populations of $1.4\text{--}1.4 M_\odot$ BNS, $10\text{--}10 M_\odot$ BBH, and $30\text{--}30 M_\odot$ BBH systems. In Fig-

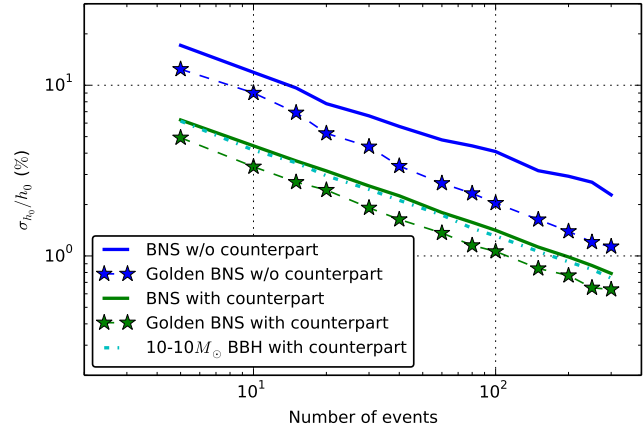


FIG. 2: Fractional error for H_0 measurement as a function of the number of events detected by HLV at design sensitivity, where σ_{h_0} is defined as half the width of the symmetric 68% credible interval. We note that golden BNS events constitute $\sim 10\%$ of the entire population, so to measure 10 golden events is the equivalent of 100 BNS events. At a projected rate of ~ 32 BNS per year (albeit with very large uncertainties), it will take a few years to progress along these curves. For the counterpart curves, we have started with a 15% prior measurement on H_0 , representing the constraint from GW170817 [1]. All other curves use a flat prior in the range 50-100 km/s/Mpc, which corresponds to $\sigma_{h_0}/h_0 = 21\%$. The amplitudes of the curves and the ratio between them varies for different observing runs.

ure 2 we demonstrate how the fractional H_0 uncertainty scales with the number of BNS events detected by HLV at design sensitivity, for both the counterpart and statistical case. We stress that the amplitude of the curves in Figure 2, as well as the relative amplitude between them, varies for different detector sensitivities and configurations, so that the ratio of the golden to the all-event curves is not constant between different observing runs. In all the counterpart curves we have started with a 15% prior measurement on H_0 , representing the constraint from GW170817 [1]; we approximate this by a Gaussian centered at 67.8 km/s/Mpc with a standard deviation of 10.2 km/s/Mpc, but the exact center and shape of the H_0 posterior do not affect our results. In the statistical curves, we have started with a flat prior on H_0 from 50 to 100 km/s/Mpc. For a single event, the H_0 posterior PDF is highly non-Gaussian due to the non-Gaussianity of the GW distance posterior PDF (due to the inclination-distance degeneracy face-on binaries have a tail to small distances, and thus high values of H_0 , while edge-on events have a tail to large distances, resulting in a tail to small values of H_0). However, after combining ~ 5 events, the H_0 measurement approaches a Gaussian and we can summarize its precision by the 1σ standard deviation. Roughly speaking, the average BNS+counterpart standard siren system constrains H_0 to 15%; although individual systems

generally do much worse than this (GW170817 was unusually close, and provided unusually good constraints), the convergence rapidly approaches $15\%/\sqrt{N}$ because of the non-Gaussian shape of the posteriors in distance and H_0 . Similarly, for golden BNS standard sirens without a counterpart, the statistical measurement of H_0 converges as roughly $20\%/\sqrt{N}$, while for the average statistical system the convergence is $\sim 40\%/\sqrt{N}$.

As expected, events with a counterpart yield the tightest H_0 constraints, and golden BNS events with a counterpart provide tighter measurements than all events. This can be seen by the difference between the solid and starred green curve in Figure 2. Meanwhile, if $10\text{--}10\ M_\odot$ BBH events have counterparts, they yield slightly better constraints than the BNS case for the same number of detections (see the cyan dot-dashed line in Figure 2). While it is unlikely that EM counterparts to BBHs exist, it may, for example, be possible to associate some mergers with a unique type of galaxy [34]. The BBH detections tend to be at farther distances for the same SNR, so if they have detectable counterparts, we expect them to yield tighter H_0 constraints because the peculiar velocity contribution will be smaller than for equivalent BNS systems. However, the majority of both BBH and BNS events are dominated by GW distance uncertainties, with peculiar velocity uncertainties remaining sub-dominant. We note that in the counterpart case, events with relatively large H_0 uncertainty still contribute significantly to the measurement. A quieter edge-on source may yield a wide H_0 measurement, but with a tail to low H_0 values, and thus can substantially tighten the H_0 constraints when combined with the measurement from a loud, face-on event with a tail to high H_0 values. The posterior distribution asymptotes to the expected $1/\sqrt{N}$ behavior after ~ 5 detections (see also the discussion in [12]). This can be seen by the slope of the curves in Figure 2, which is $1/2$. We also note that each curve in Fig. 2 is an average over 100 realizations. Since some individual detections give much tighter H_0 constraints than others, the order in which we get the detections will affect the specific rate of convergence. In an individual realization, we may get lucky in the first few events and get a very good H_0 measurement, after which we will converge more slowly than $1/\sqrt{N}$ for some time as we detect average events. After ~ 20 events, however, we reach the expected \sqrt{N} behavior for all realizations. At this point, we have a sufficient statistical sample of detections to have converged to a representative σ_{h_0} for the population, so that the convergence is mainly governed by the number of additional events rather than the order in which we detect exceptionally good events.

In cases where we cannot identify a counterpart, a golden event can yield a much better H_0 constraint than an average event. This is encapsulated in the difference between the two top curves in Fig. 2. In the extreme case, an event may have a small enough 3D localization region such that only the true host galaxy remains within [19], and the system effectively becomes a “counterpart” case.

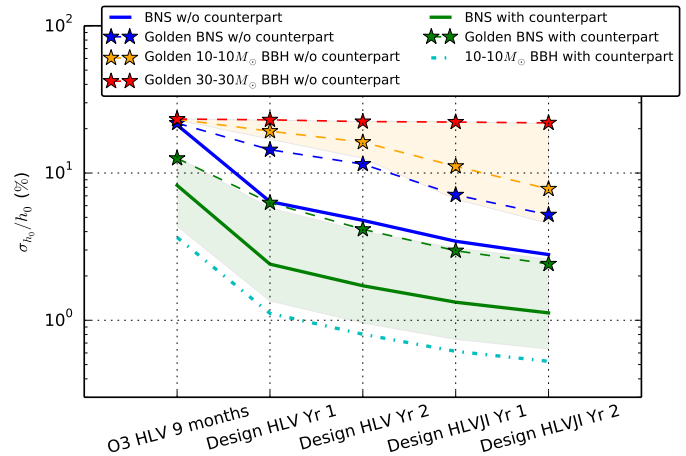


FIG. 3: Fractional error for H_0 measurement, for a range of detector networks and detector sensitivities. For the counterpart curves, we have started with a 15% prior measurement on H_0 , representing the constraint from GW170817 [1]. The H_0 prior for the other curves is uniform in the range $50\text{--}100\text{ km/s/Mpc}$. The green shaded band corresponds to the BNS rate uncertainty; the same rate uncertainty applies to the other BNS curves (green and blue). The orange shaded band corresponds to the rate uncertainty for $10\text{--}10\ M_\odot$ BBHs; the same rate uncertainty applies to the other $10\text{--}10\ M_\odot$ BBH curve (dashed light blue). Golden BNSs are those localized to within $1,000\text{ Mpc}^3$ (90% credible region), while golden BBHs are those localized to within $10,000\text{ Mpc}^3$. For the “BNS with counterpart” case (green shaded region) we find that binary neutron star standard sirens with counterparts can be expected to provide a 1% measurement by the 2nd year of HLV/JI operation ($\sim 2026+$), but given the rate uncertainties this may happen many years later or as early as the 2nd year of HLV operation ($\sim 2023+$).

We also estimate how many detections might be expected for various detector networks, and the resulting H_0 measurement uncertainty. As the network improves, the rate of detections will increase. The fraction of events with well-constrained sky positions will also increase, although the fraction of events with small localization *volumes* will not necessarily increase because there are more detections at larger distances [19]. We also expect an improvement in the fractional distance uncertainties as the number of detectors increases, as the improved polarization information may provide tighter inclination, and therefore distance, constraints.

We assume a 9-month observing season for O3 and a one-year and two-year observing season at design sensitivity [25], and take the combined duty cycle to be 0.5 for HLV and 0.3 for HLV/JI. We predict the number of detections at each observing stage according to the BBH rates published in [35] and the BNS rates in [36], namely: BNS, $10\text{--}10\ M_\odot$ BBH, and $30\text{--}30\ M_\odot$ BBH rates of 1540^{+3200}_{-1220} , 80^{+90}_{-70} , and $11^{+13}_{-10}\text{ Gpc}^{-3}\text{yr}^{-1}$ respectively. We assume the BBH mass function follows a Salpeter power law and use $10\text{--}10\ M_\odot$ BBHs to characterize all BBHs with pri-

mary component masses between 5 and 15 M_\odot , and 30–30 M_\odot BBHs to characterize all BBHs with primary component masses between 20 and 50 M_\odot . We do not place additional cuts on the secondary masses, which are distributed uniformly between 5 M_\odot and the primary mass. The number of detections is subject to Poisson statistics, and we simulate detections according to the merger rate, network sensitivity, observing time, and duty cycle. This corresponds to on average 4 (9 months)/32 (per year)/39 (per year) BNS detections at O3/HLV design/HLVJI design. At each observing stage, we combine the detections from all previous observing stages into a measurement of H_0 for each case. We repeat each simulation 100 times and report the average fractional H_0 error over all repetitions. We consider a range of sources: BNS with counterparts, BNS statistical (no counterparts; galaxy catalogs), BBH with counterparts, and BBH statistical. We note that NSBH sources are also to be expected [37–39], and these are detectable both by ground-based GW detectors and are likely to have detectable EM counterparts. Since the rates remain very uncertain, and are generally expected to be low, we do not include them in this analysis. We note that since these systems will be seen to greater distances than BNS systems, they are a potentially interesting population of GW+EM counterpart sources.

We find that if we can identify an EM counterpart and corresponding host galaxy for all BNS detections, we expect to reach a 3% measurement of H_0 after one year with a three-detector network operating at design sensitivity. Meanwhile, if BBHs have detectable counterparts, they would enable a very tight H_0 measurement, because of their high detection rates and the fact that they are almost always at large distances where peculiar velocities are negligible. However, this remains speculative, and even if some BBHs have detectable counterparts, it is likely only a small subset. Given the large uncertainties in the rates, there is also a large uncertainty in the values in Figure 3. For example, considering the 95% upper (5% lower) limit on the BNS rate results in a H_0 uncertainty of 1% (4%) after two years of Design HLV operation.

Even if we assume that only the golden BNS systems will have an unambiguous counterpart detection, we will reach a $\sim 3\%$ H_0 measurement within the second year of observation of the HLVJI network. We can also anticipate a situation in which we have a counterpart detection but no unambiguous host association. For example, an optical counterpart could be relatively isolated on the sky, with no clear nearby galaxy to be identified as the associated host. As discussed above, in this case we can pursue a pencil-beam strategy focusing on the volume within ~ 1 Mpc of the counterpart. For BNS systems, this will generally correspond to a sky area of $\lesssim 1 \text{ deg}^2$, and therefore significantly reduces the potential number of galaxy hosts and improves the power of the statistical approach (BNS detections are generally localized within $\mathcal{O}(10) \text{ deg}^2$, depending on the observing run [19]). In addition, the reduced sky area facilitates the observa-

tional task of producing a relevant catalog of galaxies. The pencil-beam case is similar to the golden case without counterparts, as it is a direct reduction in the 3D localization volumes, and thus leads to roughly similar improvements.

It is to be noted that our measurements of distance do not use any astrophysical priors, and therefore marginalize over all possible inclination angles. However, associated electromagnetic observations (for example from short GRB afterglows or jet breaks) can provide additional constraints on the inclination, and thereby improve the individual measurements of H_0 [1, 40]. In this sense our counterpart results can be considered a conservative estimate. However, one of the great advantages of standard sirens is that they are “pure”, avoiding complicated astrophysical distance ladders or poorly understood calibration processes, and instead are calibrated directly by the theory of general relativity to cosmological distances. By introducing additional constraints based on astronomical observations (e.g., independent beaming measurements or estimates of the mass distribution or equation-of-state of neutron stars), there is the potential to introduce systematic biases that could fundamentally contaminate these standard siren measurements. In the present analysis we do not consider these additional constraints, although they may indeed have an important role to play in future standard siren science.

In cases where we lack a counterpart, the H_0 measurement from all events is only a factor of ~ 2 better than the measurement restricted to only golden events, although the latter comprise $\sim 10\%$ of all events. Considering the difficulty of constructing a complete galaxy catalog for a large volume, this suggests an approach which focuses on the best-localized events for the statistical H_0 measurement. We can also carry out the statistical approach for BBHs, although very few BBHs will be well-localized in volume. We do not expect there to be enough BBHs localized to within 1,000 Mpc^3 to get meaningful H_0 constraints from these BBHs alone. If we construct a real-time galaxy catalog for all light (10–10 M_\odot) BBHs localized to within 10,000 Mpc^3 (ten times the volume of the golden BNS events), the statistical approach may provide comparable H_0 constraints to the BNS statistical approach restricted to golden BNS systems, but only if the BBH rates are on the high end (lower end of the orange shaded band in Figure 3). Meanwhile, if we constructed complete galaxy catalogs for all BNSs localized to within 10,000 Mpc^3 and carried out the statistical H_0 measurement, we would get within a factor of ~ 1.3 of the statistical measurement using all BNS systems. Thus, even in the absence of a BNS counterpart, the statistical approach for BNSs is likely to be more successful than for light BBHs. Similarly, the statistical approach for massive (30–30 M_\odot) BBHs is unlikely to provide H_0 constraints that are competitive with the BNS constraints, even if we assume that all BNS sources lack counterparts, since massive BBHs have even larger localization volumes than light BBHs, and result in too many potential host

galaxies in their 3D localization volumes.

IV. DISCUSSION

Gravitational wave standard sirens are a promising tool for measuring the Hubble constant, as emphatically shown by GW170817 [1]. We have explored how well we expect to constrain H_0 from GW standard sirens both with (“counterpart”) and without (“statistical”) direct electromagnetic measurements of the source redshift. In the counterpart case, the redshift could come either directly from an EM counterpart (e.g., from associated kilonova emission [41–44]), or through a unique host galaxy identification [1]. In the statistical case, the redshifts of all potential host galaxies within the 3D localization regions are incorporated.

We find that, if it is possible to independently measure the redshift for all BNS events, the fractional uncertainty on H_0 will reach 3% (at the 1σ level) within the first observing season of the HLV network operating at design sensitivity. After $\mathcal{O}(100)$ BNS events, GW standard sirens will provide a sub-percent determination of H_0 . This is expected to happen after ~ 2 years of operation of the full HLVJI network (~ 2026), but given the rate uncertainties could happen many years later, or could happen as early as the second year of the HLV network operating at design sensitivity (~ 2023). These results are in rough agreement with [12], which found that 15 detections by HLV at design sensitivity would constrain H_0 to 2.5% [51]. By comparison, we find that it will take ~ 20 – 30 detections at design HLV to reach 2.5%, which is generally consistent considering that we are also including the effects of peculiar velocity uncertainties. Eventually systematic errors in the amplitude calibration of the detectors may become a source of concern, as the luminosity distance is encoded in the amplitude of the GW signal. However, the calibration uncertainty is currently limited by the photon calibrator to $\sim 0.5\%$, and this is likely to improve [45]; we look forward to an era where sub-percent calibration becomes a necessity, but this is a number of years away.

If it is not possible to measure counterparts for some subset of BNS events, we can still carry out a statistical approach either for all events, or for a subset of golden events for which it is easier to construct complete galaxy catalogs. With the statistical approach, we would need more than ~ 200 BNS detections to reach a 3% H_0 measurement, or ~ 40 golden BNS systems. This may happen within the first year of HLVJI operation if using all BNS systems, or may take more than 2 years of operation if using only the golden BNS detections. We can also carry out the statistical approach for BBH systems. However, these systems (especially the more massive binaries) tend to have larger localization volumes and hence many

more potential host galaxies, so that even if we consider all BBHs localized to within $10,000 \text{ Mpc}^3$ for the statistical measurement, we will likely only get within a factor of 1.5 of the statistical constraint from golden BNS systems. We note that the constraints from statistical BBH standard sirens improve if the BBH rates are on the high end, as well as if the BBH mass function favors low masses.

We stress that our projected H_0 constraints are subject to several important uncertainties, the largest one of which is the merger rate of BNS and BBH systems. The detection rates for BBHs, as well as the fraction of well-localized events, depends sensitively on the mass distribution, which is not currently well-constrained [46, 47]. With future detections, we will have a better understanding of the merger rates and mass distributions of compact objects, which will allow for improved predictions. Regardless, it is clear that GW standard sirens, especially the well-localized, “golden” events and those with EM counterparts, will provide percent-level constraints on H_0 in the upcoming advanced detector era of GW astronomy.

Acknowledgments

We acknowledge valuable and extensive discussions with Lindy Blackburn, Reed Essick, Will Farr, and Jonathan Gair. The authors were partially supported by NSF CAREER grant PHY-1151836 and NSF grant PHY-1708081. They were also supported by the Kavli Institute for Cosmological Physics at the University of Chicago through NSF grant PHY-1125897 and an endowment from the Kavli Foundation. The authors acknowledge the University of Chicago Research Computing Center for support of this work. HYC was supported in part by the Black Hole Initiative at Harvard University, through a grant from the John Templeton Foundation. MF was supported by the NSF Graduate Research Fellowship Program under grant DGE-1746045.

Appendix A: Statistical Model

For a single event with GW and EM data, d_{GW} and d_{EM} , we can write the likelihood as:

$$p(d_{\text{GW}}, d_{\text{EM}} | H_0) = \frac{\int p(d_{\text{GW}}, d_{\text{EM}}, D_L, \alpha, \delta, z | H_0) dD_L d\alpha d\delta dz}{\beta(H_0)}, \quad (\text{A1})$$

where we have included a normalization term in the denominator, $\beta(H_0)$, to ensure that the likelihood integrates to unity. We can factor the numerator in Eq. A1 as:

$$\begin{aligned}
& \int p(d_{\text{GW}}, d_{\text{EM}}, D_L, \alpha, \delta, z | H_0) dD_L d\alpha d\delta dz \\
&= \int p(d_{\text{GW}} | D_L, \alpha, \delta) p(d_{\text{EM}} | z, \alpha, \delta) p(D_L | z, H_0) p_0(z, \alpha, \delta) dD_L d\alpha d\delta dz \\
&= \int p(d_{\text{GW}} | D_L, \alpha, \delta) p(d_{\text{EM}} | z, \alpha, \delta) \delta(D_L - \hat{D}_L(z, H_0)) p_0(z, \alpha, \delta) dD_L d\alpha d\delta dz \\
&= \int p(d_{\text{GW}} | \hat{D}_L(z, H_0), \alpha, \delta) p(d_{\text{EM}} | z, \alpha, \delta) p_0(z, \alpha, \delta) d\alpha d\delta dz,
\end{aligned} \tag{A2}$$

where $\hat{D}_L(z, H_0)$ denotes the luminosity distance of a source at redshift z , given a Hubble constant of H_0 and leaving all other cosmological parameters fixed to the Planck values ($\Omega_{M_0} = 0.308, \Omega_{\Lambda_0} = 0.692$) [24]. We can alternatively marginalize over these other cosmological parameters, but since most detected binaries will be at low redshifts (especially golden binaries, which lie within $z < 0.1$) the effects of other cosmological parameters on the z - D_L relation are small. The term $p(d_{\text{GW}} | D_L, \alpha, \delta)$ is the marginalized likelihood of the gravitational wave data given a compact binary source at distance D_L and sky position (α, δ) , marginalized over all other parameters. Throughout, we assume that we can construct a catalog of the potential host galaxies for each event, and take the prior $p_0(z, \alpha, \delta)$ to be a sum of Gaussian distributions centered at the measured redshifts and sky positions of the galaxies:

$$p_0(z, \alpha, \delta) \propto \sum_i N[\bar{z}^i, \sigma_z^i](z) N[\bar{\alpha}^i, \sigma_\alpha^i](\alpha) N[\bar{\delta}^i, \sigma_\delta^i](\delta). \tag{A3}$$

In practice, we ignore the uncertainties on the measured sky coordinates and treat the Gaussian distributions as δ -functions centered at the measured $\bar{\alpha}^i, \bar{\delta}^i$. We take \bar{z}^i to be the peculiar velocity-corrected redshifts, and assume a standard deviation of $c\sigma_z^i = 200$ km/s for each. In the above, we assign equal weights to each galaxy in the catalog, but if we believe that certain galaxies are a priori more likely to be GW hosts, we can assign weights accordingly. For example, we can weigh the galaxies in Eq. A3 by their stellar or star-forming luminosity, or by some assumed redshift-dependent coalescence rate of the GW sources. A critical assumption is that the sum in Eq. A3 contains the correct host galaxy. If we believe the catalog is incomplete, we must replace our prior, $p_0(z)$, with a weighted sum containing both the observed galaxies, Eq. A3—weighted by the catalog completeness at each (α, δ, z) —and a smooth, uniform-in-comoving volume distribution accounting for the unobserved galaxies.

In the case where we have an electromagnetic counterpart, the likelihood $p(d_{\text{EM}} | z, \alpha, \delta)$ picks out one of the galaxies in the catalog, so that the sum in the prior reduces to a single term corresponding to the EM-identified host galaxy. In the case where there is no electromagnetic counterpart, the EM data is uninformative, and we set the likelihood $p(d_{\text{EM}} | z, \alpha, \delta) \propto \text{constant}$. In the case where we have an electromagnetic counterpart but cannot pick out a unique host galaxy, one could consider a “pencil beam” containing all the potential host galaxies within ~ 1 Mpc in projected distance on the sky. We assume the sky position of the counterpart is perfectly measured to be $(\bar{\alpha}, \bar{\delta})$, and take the term $p(d_{\text{EM}} | z, \alpha, \delta)$ to be a top hat which picks out all of the galaxies within some angular radius, r , (corresponding to ~ 1 Mpc in projected distance) of the counterpart’s sky position. Thus, the numerator of Eq. A2 reduces to:

$$\int_{\langle(\alpha, \delta) | (\bar{\alpha}, \bar{\delta})\rangle < r} p(d_{\text{GW}} | \hat{D}_L(z, H_0), \bar{\alpha}, \bar{\delta}) p_0(z, \alpha, \delta) dz d\alpha d\delta, \tag{A4}$$

and we sum over all galaxies within ~ 1 Mpc in projected distance, but no longer weigh them by the likelihood of the GW source at the corresponding sky position. Alternatively, we can incorporate assumptions about the kick distribution in the form of $p(d_{\text{EM}} | z, \alpha, \delta)$ and place more weight at galaxies close to $(\bar{\alpha}, \bar{\delta})$ rather than assuming a simple top hat. Although for simplicity we don’t apply the pencil-beam approach in §III, it can be thought of as a natural interpolation between the counterpart and statistical cases.

To calculate the normalization term, $\beta(H_0)$, in the denominator of Eq. A1, we must account for selection effects in our measurement process. In general, the GW and EM data are both subject to selection effects in that we only detect GW and EM sources that are above some threshold, $d_{\text{GW}}^{\text{th}}$ and $d_{\text{EM}}^{\text{th}}$, respectively. Accounting for these detection thresholds, the denominator of Eq. A1 is:

$$\beta(H_0) = \int_{d_{\text{EM}} > d_{\text{EM}}^{\text{th}}} \int_{d_{\text{GW}} > d_{\text{GW}}^{\text{th}}} \int^4 p(d_{\text{GW}}, d_{\text{EM}}, D_L, \alpha, \delta, z | H_0) dD_L dz d\alpha d\delta dd_{\text{GW}} dd_{\text{EM}} \tag{A5}$$

We define:

$$p_{\text{det}}^{\text{GW}}(D_L, \alpha, \delta) \equiv \int_{d_{\text{GW}} > d_{\text{GW}}^{\text{th}}} p(d_{\text{GW}} | D_L, \alpha, \delta) dd_{\text{GW}}, \quad (\text{A6})$$

and similarly:

$$p_{\text{det}}^{\text{EM}}(z, \alpha, \delta) \equiv \int_{d_{\text{EM}} > d_{\text{EM}}^{\text{th}}} p(d_{\text{EM}} | z, \alpha, \delta) dd_{\text{EM}}. \quad (\text{A7})$$

With these definitions, Eq. A5 becomes:

$$\beta(H_0) \quad (\text{A8})$$

$$= \int p_{\text{det}}^{\text{GW}}(\hat{D}_L(z, H_0), \alpha, \delta) p_{\text{det}}^{\text{EM}}(z, \alpha, \delta) p_0(z, \alpha, \delta) d\alpha d\delta dz. \quad (\text{A9})$$

Note that we have applied the same chain-rule factorization to the inner four integrals as in Eq. A2. It is clear that the normalization factor $\beta(H_0)$ depends on H_0 , so it is crucial to include it in the likelihood. For the EM selection effects, we assume that we can detect all EM counterparts and host galaxies up to some maximum true redshift, z_{max} . This is an over-simplification of the true EM selection effects, but is a reasonable assumption for the real-time galaxy catalogs that will be constructed during the EM follow-up to GW events. For example, at design aLIGO sensitivity, 90% of 30–30 M_{\odot} BBH detections will be within 5 Gpc (and BNS detections will be within 0.3 Gpc) [48][52]. Furthermore, we argue that if BBHs lack counterparts, the golden BBH detections, which will typically be within 400 Mpc, yield tighter H_0 constraints than the majority of BBHs (and the golden BNS events yield even tighter constraints, even if they lack counterparts). Thus, the events that are easier to follow up (because they are closer and have smaller GW localization volumes) also contribute more to the H_0 measurement. A galaxy with the same absolute magnitude as the Milky Way would have an apparent magnitude of $\lesssim 23$ at typical 30–30 M_{\odot} BBH distances, or $\lesssim 17.5$ for golden BBHs, and $\lesssim 17$ at typical BNS distances. Meanwhile, we expect kilonova counterparts to BNS mergers to have magnitudes of ≤ 21.7 on the first night, even at the farthest distances detectable by the HLVJI network at design sensitivity (assuming the optical counterpart to GW170817 is typical; [41, 49]). This is well within the magnitude limits of upcoming survey telescopes (e.g. LSST), as well as within reach of current instruments (e.g. DECam, Subaru Hyper Suprime-Cam, ZTF etc.).

We assume that EM counterparts are detectable for binaries regardless of the binary inclination. Although the GRB emission is expected to be beamed, the associated kilonovae are expected to emit isotropically. Furthermore, as GW170817 demonstrated, it is possible to identify a kilonova counterpart independently of the GRB. We note that since face-on/face-off binaries are louder than edge-on binaries in GWs, the population of detected binaries will show a preference for face-on/face-off; our

analysis reproduces the expected inclination distribution among detected sources (see Fig. 4 of [50]). Under these assumptions for the EM selection effects, we have:

$$p_{\text{det}}^{\text{EM}}(z, \alpha, \delta) \propto \mathcal{H}(z_{\text{max}} - z), \quad (\text{A10})$$

where \mathcal{H} is the Heaviside step function, and Eq. A8 reduces to:

$$\beta(H_0) = \quad (\text{A11})$$

$$\int_0^{z_{\text{max}}} \int \int p_{\text{det}}^{\text{GW}}(\hat{D}_L(z, H_0), \alpha, \delta) p_0(z, \alpha, \delta) d\alpha d\delta dz. \quad (\text{A12})$$

Meanwhile, we assume that the galaxy distribution is approximately isotropic on large scales, so that the galaxy catalog prior can be factored as:

$$p_0(z, \alpha, \delta) \approx p_0(z) p_0(\alpha, \delta), \quad (\text{A13})$$

and we approximate $p_0(\alpha, \delta)$ by a continuous, isotropic distribution on the sky. We note that this assumption would only introduce systematic errors if the galaxy distribution had significant correlations with the sky sensitivities of the detectors, which is not to be expected. We then define:

$$p_{\text{det}}^{\text{GW}}(D_L) = \int p_{\text{det}}^{\text{GW}}(D_L, \alpha, \delta) p_0(\alpha, \delta) d\alpha d\delta. \quad (\text{A14})$$

We assume a detection threshold for GW sources corresponding to a matched-filter network SNR $\rho_{\text{th}} = 12$, so that the detection probability, $p_{\text{det}}^{\text{GW}}(D_L)$, is the probability that a source at distance D_L will have SNR $\rho > 12$. The network SNR can be calculated for a source at a given distance, sky position, orientation, component masses and spins. Assuming a distribution of orientations, masses and spins among a population of sources, in addition to the assumed isotropic distribution on the sky, $p_0(\alpha, \delta)$, we calculate the fraction of sources that are detectable at a given distance, $p_{\text{det}}^{\text{GW}}(D_L)$. We assume an isotropic distribution of orientation angles, and fix spins to be zero. For simplicity, we assume a monochromatic mass distribution for each type of source. (For example, we take all BNS sources to be 1.4–1.4 M_{\odot} .)

We therefore have:

$$\beta(H_0) = \int_0^{z_{\text{max}}} p_{\text{det}}^{\text{GW}}(D_L(z, H_0)) p_0(z) dz. \quad (\text{A15})$$

We note that for GW sources in the local universe ($D_L \lesssim 50$ Mpc),

$$\hat{D}_L(z, H_0) \approx \frac{cz}{H_0}. \quad (\text{A16})$$

If we assume that the distribution of galaxies is uniform in comoving volume, then in the local universe, we can approximate:

$$p_0(z) \propto z^2. \quad (\text{A17})$$

With these approximations, assuming that EM selection effects are negligible ($z_{\max} \rightarrow \infty$), $\beta(H_0)$ is independent of the masses of the source, which determine the distance to which it can be detected. In fact, under these assumptions, $\beta(H_0)$ simplifies to:

$$\beta(H_0) \propto H_0^3. \quad (\text{A18})$$

However, in general, we must account for cosmological deviations from Eqs. A16 and A17 so we calculate $\beta(H_0)$

according to Eq. A15 throughout our analysis. We note that $\beta(H_0)$ is still only weakly dependent on the GW horizon and therefore the (unknown) underlying mass distribution of GW sources. Nevertheless, the statistical framework described here can accommodate more complicated models of the GW source distribution and its effects on the detection probability (Eq. A14) as well as the galaxy catalog completeness function (Eq. A3 and Eq. A10).

-
- [1] B. P. Abbott, R. Abbott, T. D. Abbott, F. Acernese, K. Ackley, C. Adams, T. Adams, P. Addesso, R. X. Adhikari, V. B. Adya, et al., *Nature (London)* **551**, 85 (2017), 1710.05835.
 - [2] B. P. Abbott, R. Abbott, T. D. Abbott, F. Acernese, K. Ackley, C. Adams, T. Adams, P. Addesso, R. X. Adhikari, V. B. Adya, et al., *Physical Review Letters* **119**, 161101 (2017), 1710.05832.
 - [3] B. F. Schutz, *Nature (London)* **323**, 310 (1986).
 - [4] D. F. Chernoff and L. S. Finn, *Astrophys. J. Lett.* **411**, L5 (1993), gr-qc/9304020.
 - [5] C. Messenger and J. Read, *Physical Review Letters* **108**, 091101 (2012), 1107.5725.
 - [6] D. E. Holz and S. A. Hughes, *Astrophys. J.* **629**, 15 (2005), URL <http://stacks.iop.org/0004-637X/629/i=1/a=15>.
 - [7] N. Dalal, D. E. Holz, S. A. Hughes, and B. Jain, *Phys. Rev. D* **74**, 063006 (2006), astro-ph/0601275.
 - [8] B. P. Abbott, R. Abbott, T. D. Abbott, F. Acernese, K. Ackley, C. Adams, T. Adams, P. Addesso, R. X. Adhikari, V. B. Adya, et al., *Astrophys. J. Lett.* **848**, L13 (2017), 1710.05834.
 - [9] C. Cutler and D. E. Holz, *Phys. Rev. D* **80**, 104009 (2009), 0906.3752.
 - [10] J. S. Bloom, D. E. Holz, S. A. Hughes, K. Menou, A. Adams, S. F. Anderson, A. Becker, G. C. Bower, N. Brandt, B. Cobb, et al., *ArXiv e-prints* (2009), 0902.1527.
 - [11] S. Nissanke, D. E. Holz, S. A. Hughes, N. Dalal, and J. L. Sievers, *Astrophys. J.* **725**, 496 (2010), 0904.1017.
 - [12] S. Nissanke, D. E. Holz, N. Dalal, S. A. Hughes, J. L. Sievers, and C. M. Hirata, *ArXiv e-prints* (2013), 1307.2638.
 - [13] A. Nishizawa, *ArXiv e-prints* (2016), 1612.06060.
 - [14] N. Seto and K. Kyutoku, *ArXiv e-prints* (2017), 1710.06424.
 - [15] W. Del Pozzo, *Phys. Rev. D* **86**, 043011 (2012), 1108.1317.
 - [16] C. Messenger, K. Takami, S. Gossan, L. Rezzolla, and B. S. Sathyaprakash, *Physical Review X* **4**, 041004 (2014), 1312.1862.
 - [17] W. Del Pozzo, T. G. F. Li, and C. Messenger, *Phys. Rev. D* **95**, 043502 (2017), 1506.06590.
 - [18] H.-Y. Chen and D. E. Holz, *ArXiv e-prints* (2014), 1409.0522.
 - [19] H.-Y. Chen and D. E. Holz, *ArXiv e-prints* (2016), 1612.01471.
 - [20] W. Hu, in *Observing Dark Energy*, edited by S. C. Wolff and T. R. Lauer (2005), vol. 339 of *Astronomical Society of the Pacific Conference Series*, p. 215, astro-ph/0407158.
 - [21] W. L. Freedman, *Nature Astronomy* **1**, 0121 (2017).
 - [22] B. P. Abbott, R. Abbott, T. D. Abbott, M. R. Abernathy, F. Acernese, K. Ackley, C. Adams, T. Adams, P. Addesso, R. X. Adhikari, et al., *Living Reviews in Relativity* **19**, 1 (2016), 1304.0670.
 - [23] H.-Y. Chen, D. E. Holz, J. Miller, M. Evans, S. Vitale, and J. Creighton, *ArXiv e-prints* (2017), 1709.08079.
 - [24] P. A. R. Ade, N. Aghanim, M. Arnaud, M. Ashdown, J. Aumont, C. Baccigalupi, A. J. Banday, R. B. Barreiro, J. G. Bartlett, and et al., *Astron. Astrophys.* **594**, A13 (2016), 1502.01589.
 - [25] B. P. Abbott, R. Abbott, T. D. Abbott, M. R. Abernathy, F. Acernese, K. Ackley, C. Adams, T. Adams, P. Addesso, R. X. Adhikari, et al., *Living Reviews in Relativity* **19**, 1 (2016), 1304.0670.
 - [26] J. Veitch, V. Raymond, B. Farr, W. Farr, P. Graff, S. Vitale, B. Aylott, K. Blackburn, N. Christensen, M. Coughlin, et al., *Phys. Rev. D* **91**, 042003 (2015), 1409.7215.
 - [27] J. Carrick, S. J. Turnbull, G. Lavaux, and M. J. Hudson, *Mon. Not. R. Astron. Soc.* **450**, 317 (2015), 1504.04627.
 - [28] D. M. Scolnic, D. O. Jones, A. Rest, Y. C. Pan, R. Chornock, R. J. Foley, M. E. Huber, R. Kessler, G. Narayan, A. G. Riess, et al., *ArXiv e-prints* (2017), 1710.00845.
 - [29] P. Schechter, *Astrophys. J.* **203**, 297 (1976).
 - [30] P. Norberg, S. Cole, C. M. Baugh, C. S. Frenk, I. Baldry, J. Bland-Hawthorn, T. Bridges, R. Cannon, M. Colless, C. Collins, et al., *Mon. Not. R. Astron. Soc.* **336**, 907 (2002), astro-ph/0111011.
 - [31] J. Liske, D. J. Lemon, S. P. Driver, N. J. G. Cross, and W. J. Couch, *Mon. Not. R. Astron. Soc.* **344**, 307 (2003), astro-ph/0207555.
 - [32] R. E. González, M. Lares, D. G. Lambas, and C. Valotto, *Astron. Astrophys.* **445**, 51 (2006), astro-ph/0507144.
 - [33] E. Kourkchi and R. B. Tully, *Astrophys. J.* **843**, 16 (2017), 1705.08068.
 - [34] A. Loeb, *Astrophys. J. Lett.* **819**, L21 (2016), 1602.04735.
 - [35] B. P. Abbott, R. Abbott, T. D. Abbott, M. R. Abernathy, F. Acernese, K. Ackley, C. Adams, T. Adams, P. Addesso, R. X. Adhikari, et al. (LIGO Scientific and Virgo Collaboration), *Phys. Rev. Lett.* **118**, 221101 (2017), URL <https://link.aps.org/doi/10.1103/PhysRevLett.118.221101>.
 - [36] B. P. Abbott, R. Abbott, T. D. Abbott, F. Acernese, K. Ackley, C. Adams, T. Adams, P. Addesso, R. X. Adhikari, V. B. Adya, et al. (LIGO Scientific Col-

- laboration and Virgo Collaboration), *Phys. Rev. Lett.* **119**, 161101 (2017), URL <https://link.aps.org/doi/10.1103/PhysRevLett.119.161101>.
- [37] M. Dominik, E. Berti, R. O’Shaughnessy, I. Mandel, K. Belczynski, C. Fryer, D. E. Holz, T. Bulik, and F. Panarale, *Astrophys. J.* **806**, 263 (2015), 1405.7016.
 - [38] K. Belczynski, S. Repetto, D. E. Holz, R. O’Shaughnessy, T. Bulik, E. Berti, C. Fryer, and M. Dominik, *Astrophys. J.* **819**, 108 (2016), 1510.04615.
 - [39] K. Belczynski, D. E. Holz, T. Bulik, and R. O’Shaughnessy, *Nature (London)* **534**, 512 (2016), 1602.04531.
 - [40] C. Guidorzi, R. Margutti, D. Brout, D. Scolnic, W. Fong, K. D. Alexander, P. S. Cowperthwaite, J. Annis, E. Berger, P. K. Blanchard, et al., *ArXiv e-prints* (2017), 1710.06426.
 - [41] M. Soares-Santos, D. E. Holz, J. Annis, R. Chornock, K. Herner, E. Berger, D. Brout, H.-Y. Chen, R. Kessler, M. Sako, et al., *Astrophys. J. Lett.* **848**, L16 (2017), 1710.05459.
 - [42] P. S. Cowperthwaite, E. Berger, V. A. Villar, B. D. Metzger, M. Nicholl, R. Chornock, P. K. Blanchard, W. Fong, R. Margutti, M. Soares-Santos, et al., *Astrophys. J. Lett.* **848**, L17 (2017), 1710.05840.
 - [43] M. Nicholl, E. Berger, D. Kasen, B. D. Metzger, J. Elias, C. Briceño, K. D. Alexander, P. K. Blanchard, R. Chornock, P. S. Cowperthwaite, et al., *Astrophys. J. Lett.* **848**, L18 (2017), 1710.05456.
 - [44] R. Chornock, E. Berger, D. Kasen, P. S. Cowperthwaite, M. Nicholl, V. A. Villar, K. D. Alexander, P. K. Blanchard, T. Eftekhari, W. Fong, et al., *Astrophys. J. Lett.* **848**, L19 (2017), 1710.05454.
 - [45] S. Karki, D. Tuyenbayev, S. Kandhasamy, B. P. Abbott, T. D. Abbott, E. H. Anders, J. Berliner, J. Betzwieser, C. Cahillane, L. Canete, et al., *Review of Scientific Instruments* **87**, 114503 (2016), 1608.05055.
 - [46] B. P. Abbott, R. Abbott, T. D. Abbott, M. R. Abernathy, F. Acernese, K. Ackley, C. Adams, T. Adams, P. Addesso, R. X. Adhikari, et al., *Astrophys. J. Lett.* **833**, L1 (2016), 1602.03842.
 - [47] M. Fishbach and D. E. Holz, *Astrophys. J. Lett.* **851**, L25 (2017), 1709.08584.
 - [48] H.-Y. Chen, D. E. Holz, J. Miller, M. Evans, S. Vitale, and J. Creighton, *ArXiv e-prints* (2017), 1709.08079.
 - [49] B. P. Abbott, R. Abbott, T. D. Abbott, F. Acernese, K. Ackley, C. Adams, T. Adams, P. Addesso, R. X. Adhikari, V. B. Adya, et al., *Astrophys. J. Lett.* **848**, L12 (2017), 1710.05833.
 - [50] B. F. Schutz, *Classical and Quantum Gravity* **28**, 125023 (2011), 1102.5421.
 - [51] Note that [12] use the 68% credible interval to quote fractional uncertainties, whereas we use half the width of the 68% credible interval in this work.
 - [52] <http://gwcc.rcc.uchicago.edu/>